City Research Online

City St George's, University of London

Citation: Soysouvanh, S., Jalil, M. A., Amiri, I. S., Ali, J., Singh, G., Mitatha, S., Yupapin, P., Grattan, K. T. V. & Yoshida, M. (2018). Ultra-fast electro-optic switching control using a soliton pulse within a modified add-drop multiplexer. Microsystem Technologies, 24(9), pp. 3777-3782. doi: 10.1007/s00542-018-3837-y

This is the accepted version of the paper.

This version of the publication may differ from the final published version. To cite this item please consult the publisher's version.

Permanent repository link: https://openaccess.city.ac.uk/id/eprint/19765/

Link to published version: https://doi.org/10.1007/s00542-018-3837-y

Copyright and Reuse: Copyright and Moral Rights remain with the author(s) and/or copyright holders. Copies of full items can be used for personal research or study, educational, or not-for-profit purposes without prior permission or charge, unless otherwise indicated, provided that the authors, title and full bibliographic details are credited, a hyperlink and/or URL is given for the original metadata page and the content is not changed in any way. For full details of reuse please refer to City Research Online policy.

City Research Online: http://openaccess.city.ac.uk/ publications@citystgeorges.ac.uk

Ultra-fast Electro-optic Switching Control using a Soliton Pulse within a Modified Add-drop Multiplexer

S. Soysouvanh[1], M.A. Jalil[2], I.S. Amiri[3], J. Ali[4], G. Singh[5], S. Mitatha[1*], P. Yupapin[6, 7*], K.T.V. Grattan[8], and M. Yoshida[9]

[1]Department of Computer Engineering, Faculty of Engineering, King Mongkut's Institute of Technology Ladkrabang, Bangkok, 10520, Thailand;
[2]Department of Physics, Faculty of Science, Universiti Teknologi Malaysia, 81310 Johor Bahru Malaysia, 81300 Johor Bahru, Malaysia;
[3]Division of Materials Science and Engineering, Boston University, Boston, MA, 02215, USA;
[4]Laser Center, IbnuSina Institute for Industrial and Scientific Research, UniversitiTeknologi Malaysia (UTM)
[5]Department of Electronics and Communication Engineering, Malaviya National Institute of Technology Jaipur, 302017, India;
[6]Computational Optics Research Group, Advanced Institute of Materials Science, Ton Duc Thang University, District 7, Ho Chi Minh City, 700,000, Vietnam;
[7]Faculty of Electrical & Electronics Engineering; Ton Duc Thang University, District 7, Ho Chi Minh City, 700,000, Vietnam;
[8]Department of Electrical & Electronic Engineering, School of Mathematics, Computer Science & Engineering, The City, University of London, EC1V 0HB, United Kingdom;
[9]Department of Embedded Technology, School of Information and Telecommunication Engineering, Tokai University, 2-3-23, Takanawa, Minato-ku, Tokyo, 108-8619, Japan;
*Corresponding author E-mail:preecha.yupapin@tdt.edu.vn, kmsomsak@kmitl.ac.th

Abstract: We have proposed the use of a soliton pulse that propagates within a modified add-drop filter, which is made of a GaAsInP/P material. It is in the form of a Panda-ring resonator, from which a bright/dark soliton pulse is input into a system via an input port. The conversion between bright and dark soliton pulses is introduced at the 3dB coupler, i.e. the change in phase of $\pi/2$. But it is not superimposed each other. The output solitons obtained at the through and drop ports are bight and dark solitons respectively. Both signals can be used to form "ON' and "OFF" or "1" and "0", which are useful for the digital bit generation. The switching speed of the system can be improved by employing the two nonlinear side rings. In application, secure output bits can be arranged by using the alternative input solitons or the control ports, where the input bright and dark solitons can be converted into output bits. This means that the output bits can be randomly switched between "1" and "0", which can be identified by the sender. Moreover, the additional information can be multiplexed via the add port and transmitted in either free space or optical fiber via the whispering gallery mode and through port outputs. Finally, the electro-optic switching can be transferred and the electronic switching by the embedded stacked layers, where the ultrafast switching of light input can lead the ultrafast electrical switching speed. The switching speed of ~5 fs and the offset time of ~220 fs of the "on" and OFF" are achieved by using the selected ring parameters.

Keywords: Ultra-switching**;** Electro-optic switching; Electro-optic flip flop; S.oliton switching

1. Introduction

Electro-optic devices have progressed rapidly in the recent years due to the development of new materials that can support both optical and electrical applications such graphene [1], ZnO [2] and chalcogenide glass [3]. It has increased the trend of the electro-optic devices have increased in many areas of investigation [4-6]. One of the major investigations is the electro-optic switching that can offer many advantages for the communication devices and related technologies [7-10]. The electronic switching signal has the major role in many applications, especially in computing, communication and control systems. However, the electronic switching has the limitation in speed improvement the best electronic switching speed of ns is could be achieved until now [11]. Optical switching has shown the ability in many applications, in which the improvement has no limitation in the signal generation, while the limitation is the detection device [12-14]. The search for high-speed switching is continued, however, the improvement is rarely seen. Recently, the interesting aspect of electro-optic signal conversion has come through when the stacked layers of the silicon-graphene-gold materials have shown promising behaviors [15-17], from which the switching between light and electrical signals can be performed. The advantage of the fast switching from light signal can be transferred to the electrical signal by using a stacked layer device. The input sources via the stacked layers can be either light or electrical signals that can be transmitted and recovered at the other ends. In this case, the electronic switching speed can be improved by using the microscale device. The requirement of the ultrafast switching can be fulfilled in addition to power stability by using the soliton pulse input which has the narrow pulse width and displays stable power during the operation[18]. In this research, a soliton pulse is used for processing within the system. The alternative signals between bright and dark soliton can be obtained at the through and drop ports respectively. The ultrafast signals can also be improved by the two nonlinear side-rings. The fast electronic-switching is obtained at the gold layer interface. The control signal is provided by the Gaussian input via the add port. This article presents simulation

work The graphical method is firstly introduced, the verified results are obtained by the MATLAB program. Reality-based parameters are employed in our simulations, hence, the realization of the proposed device seems fairly possible.

2. Theoretical Background

By using the graphical method known as an Optiwave program, where all output field parameters are specified and used for MATLAB simulation by using the related equations (1)–(9). The switching output can be obtained, in which the switching time can also modify using the two nonlinear phase modulators. The transfer functions of the system ports are given by the authors in reference [19-20]. But it they are required to modify and re-arrange, especially, the changes in the propagation lengths and the coupling constants including in the propagation fields. The control signal is input into the add port that can be obtained at the drop and through port after the resonant condition. Ther is no imposed on the soliton signals and others because of the soliton pulse is not evolved with any combination input field.

The proposed waveguide material is made of a nonlinear material known as an GaAsInP/P, where the refractive index(n) is given by $n = n_0 + n_2 I = n_0 + n_2 \frac{P}{A_{eff}}$, Where n_0 and n_2 are the linear and nonlinear refractive indexes, respectively. I is the optical intensity and P is the optical power. A_{eff} is the effective mode core area of the device. For micro/nano ring resonator, the effective mode core areas range from 0.1 to 0.5 μm^2 [20]. Generally, the resonant output of the light field is the ratio between the output fields (E_{th} (t) or E_{dr} (t)) and input field (E_{in} (t)) in each roundtrip within the system without the two side phaase modulator, which is shown in Figure 1.

The transfer function of output power/intensities at through port and drop port are given by (1) and (2), respectively[19].

$$\left|E_{th}\right|^2 = \left|\frac{\tau_2 - \tau_1 A\Phi}{1-\tau_1\tau_2 A\Phi} E_{in} + \frac{-\kappa_1\kappa_2 A_{1/2}\Phi_{1/2}}{1-\tau_1\tau_2 A\Phi} E_{ad}\right|^2 \quad (1)$$

$$\left|E_{dr}\right|^2 = \left|\frac{\tau_2 - \tau_1 A\Phi}{1-\tau_1\tau_2 A\Phi} E_{ad} + \frac{-\kappa_1\kappa_2 A_{1/2}\Phi_{1/2}}{1-\tau_1\tau_2 A\Phi} E_{in}\right|^2 \quad (2)$$

Where $A_{1/2} = \exp(-\alpha L/4)$ is the half-roundtrip amplitude ($A = A_{1/2}^2$), $\Phi_{1/2} = \exp(j\omega T/2)$ is the half-roundtrip phase contribution ($\Phi = \Phi_{1/2}^2$), $\tau_{1,2} = \sqrt{1-\kappa_{1,2}^2}$, κ_1 and κ_2 are the coupling constants.

We have proposed the ultrafast switching generation system, which is required the soliton input that can provide the fast switching with power stability. When the input is the bright soliton pulse(E_B), the output at the the through and drop prorts after the time evolution are the bright abd dark(E_D)solitons, repaectively, which are given by [19, 20]

$$E_B(t) = A_0 \operatorname{sech}\left[\frac{T}{T_0}\right] \exp\left[\left(\frac{z}{2L_D}\right) - i\omega_0 t\right] \quad (3)$$

$$E_D(t) = A_0 \tanh\left[\frac{T}{T_0}\right] \exp\left[\left(\frac{z}{2L_D}\right) - i\omega_0 t\right] \quad (4)$$

Where A is the optical field amplitude and z is the propagation distance. T is the soliton propagation time in the frame moving at the group velocity ($T = t - \beta_1 z$), here β_1 and β_2 are the coefficients of the linear and second-order terms of Taylor expansion of the propagation constant. L_d is the dispersion length of the soliton pulse ($L_d = T_0^2/|\beta|$). T_0 is the initial soliton pulse width, where t is the soliton phase shift time, and ω_0 is the frequency of the soliton. This solution describes a pulse that keeps its temporal width invariance as it propagates, and thus is called a temporal soliton. When a soliton peak intensity ($\beta/\Gamma T_0^2$) is given, then T_0 is known. For the soliton pulse in the micro/nano ring device, a balance should be achieved between dispersion length (L_d) and nonlinear length ($L_{nl} = 1/\Gamma\phi_{nl}$), where Γ is the length scale over which dispersive or nonlinear effects make the beam become wider or narrower ($\Gamma = n_2 k_0$). For a soliton pulse, there is a balance between dispersion and nonlinear lengths, hence, $L_d = L_{nl}$, this is a dispersion compensation behavior os a soliton propagation.

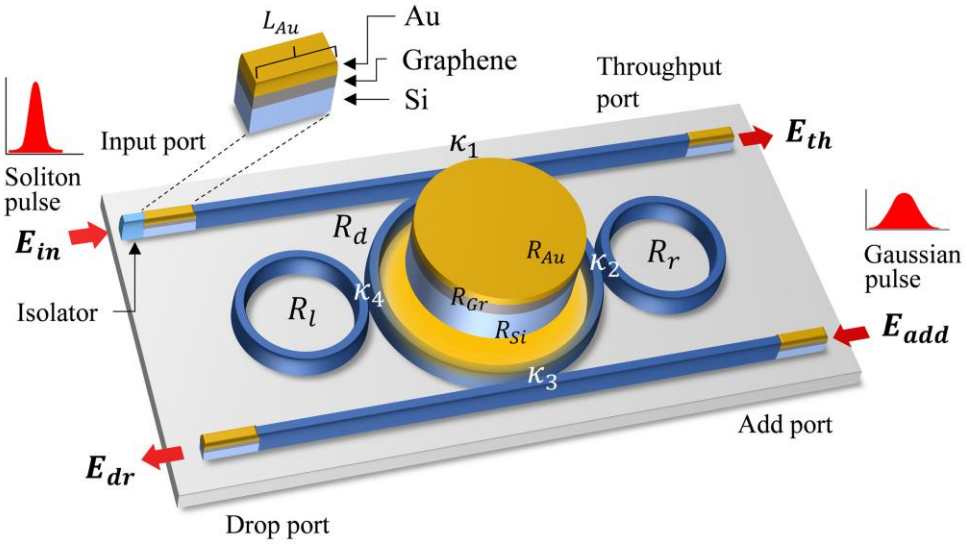

Figure 1: A schematic illustration of a Modified Add-drop Multiplexer , where R_d, R_r, R_l, are the ring radii of the center ring and two side rings, right (R_r) and left (R_l) hands, R_{Si}: Silicon ring radius, R_{Gr}: Graphene ring radius, R_{Au}: Gold ring radius. E_{in}, E_{th}, E_{dr} and E_{add} are the input port, throughput port, drop port, and add port electrical fields, respectively. The coupling constants $\kappa_1 = \kappa_2 = \kappa_3 = \kappa_4 = 0.5$. The other parameters are given by the related figure captions.

3. Simulation Results

In simulations, we started with the graphical approach. Figure 2 shows the graphical plot of the bright soliton input with a pulse spectral width of 60 nm, the center wavelength is at 1.55 micron and peak power is 1.0 W. The whispering gallery mode is obtained as shown in Figure 2, the WGM formalism can be found in the reference [21]. The used parameters in the Optiwave program are applied to the following results. The outputs at the throughput and drop ports are plotted in Fig. 3, where the switching signals are formed by the bright and dark solitons, respectively. Those two states of signals are labelled as "1" and "0" which present the binary digits or bits. Results of the drop port and throughput port signals are as shown in Figure 3, where (a) the input soliton pulse is 1 W with a center wavelength of 1.55 µm, a pulse spectral width of 60 nm at FWHM. The Gaussian pulse power is 1 W, of which the time offset is 220 fs with a half-width of 5 fs, the center wavelength is 1.55 µm with 450 nm bandwidth at FWHM, (b) the bright soliton is input into the add port, with the soliton pulse peak power is 1 W, a soliton center wavelength of 1.55 µm, the soliton spectral width is 60 nm at the full width at the half maximum(FWHM). From which the secure output bits can be obtained by using the control signal applied at the add port. In this example, the bright soliton is assigned as the control signal and input into the system. At the resonant condition, the output solitons at the throughput and drop ports change to "0" and "1" as shown in Fig. 3(b). In application, the control signals can be randomly applied either a bright or dark solitons and the sender can recognize and verify the corrected output bits(codes) with the end user.

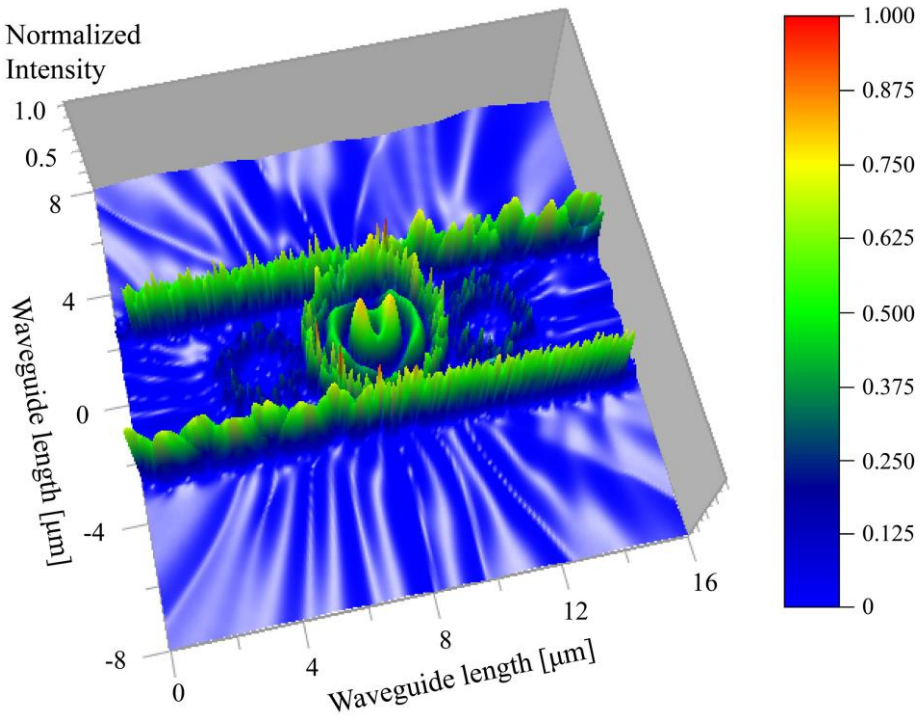

Figure 2: Plot of the result obtained by the Optiwave program, where $R_l = R_r = 1.1$ µm , $R_d = 2.0$ µm.

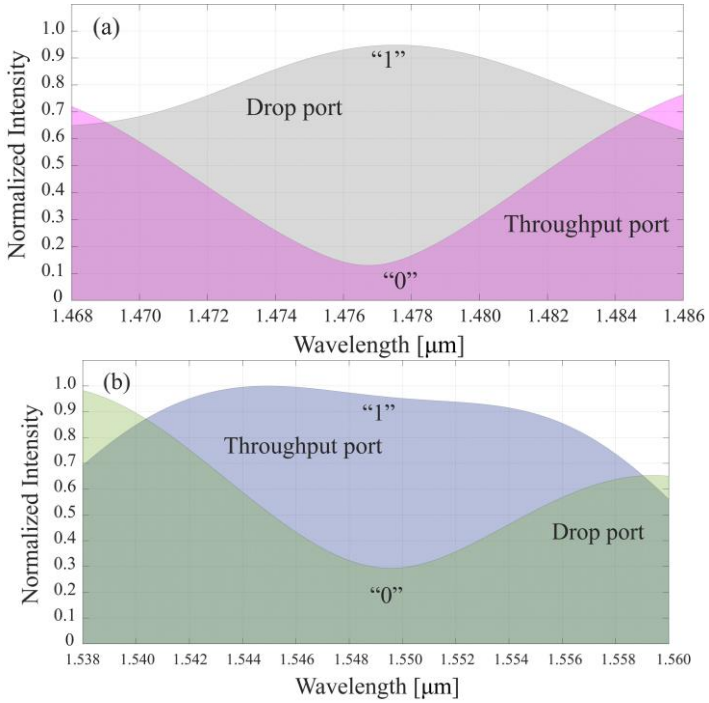

Figure 3. Results of the drop port and throughput port signals, (a) the input soliton pulse is 1 W with a center wavelength of 1.55 μm and a spectral width of 60 nm at FWHM. The Gaussian pulse is 1 W, (b) the input into the add port is the bright soliton pulse of 1 W peak power, at the center wavelength of 1.55 μm, the spectral width at FWHM is 60 nm.

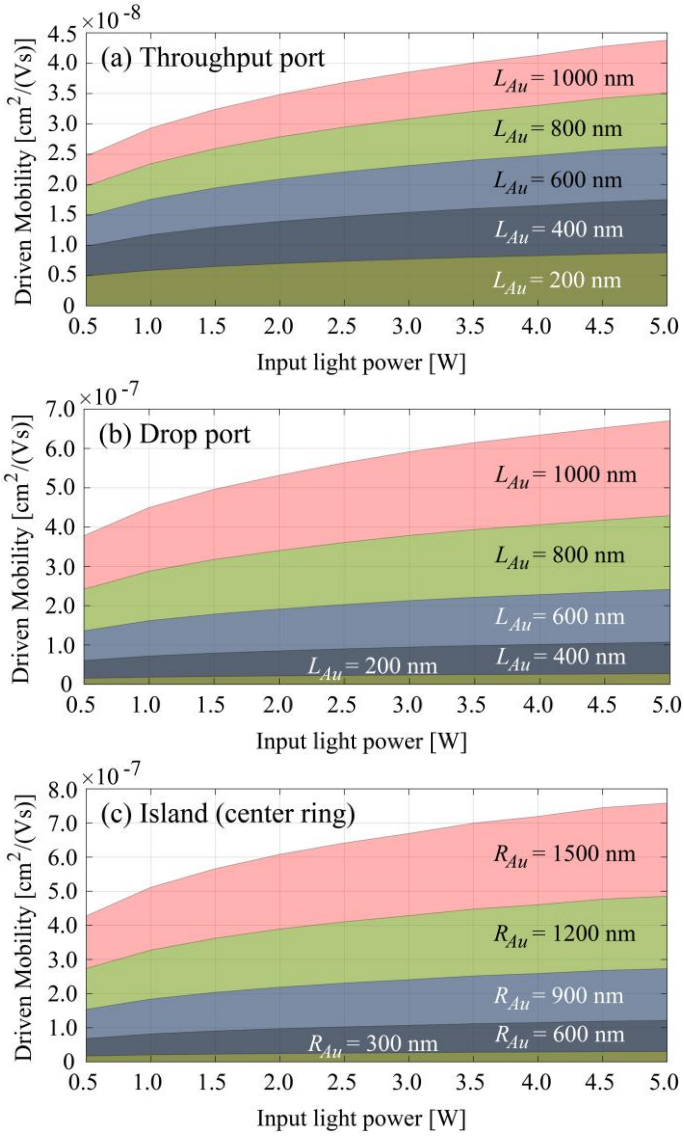

Figure 4. The plot of the mobility outputs of the system, where the gold layer parameters are w = 0.5 μm, thickness = 0.5 μm, the gold island thickness is 0.5 μm. The gold ring radii are varied from 600-1500 nm.

The mobility outputs of the stacked waveguide outputs are plotted in Fig. 4. The used parameters are w = 0.5 µm, thickness = 0.5 µm, the gold Island thickness is 0.5 µm. The output mobility and input power relationship are plotted, where (a) the throughput port, (b) drop port, and (c) the Island. The other information can also be included via the multiplexed input (add) port. The results of the multiplexed signal are shown in Figs. 5-7, where the relationship between the driven mobility of the Island and the switching time is plotted. From which the transmission links of the output signals can be employed via the free space link using the WGM outputs. In this proposed work, the transmission signals can be used in either optical or electrical form by using the stacked layers of silicon-graphene-gold, in which the conversion of the electro-optic signals can be provided. The relationship between the light intensity (I), group velocity and the electron mobility can be expressed as $\boldsymbol{I = E^2 = (\frac{V_d}{\mu})^2}$, which is defined by $V_d = \mu E$. When an electric field E is applied to the grating sensor, an electric current is established in the conductor. The density J_s of this current is given by $J_s = \sigma E$. The constant of proportionality σ is called the specific conductance or electrical conductivity of the conductor, for gold, it is 1.6×10^8 $W^{-1}m^{-1}$ [23, 24]. The electron mobility in gold is 42.6 $cm^2 V^{-1} s^{-1}$, the electron mass is 9.10×10^{-31} kilograms, the electron charge is 1.60×10^{-19} coulombs. The refractive index of the silicon is 1.46. The linear and nonlinear refractive indices of the GaAsInP/P are 3.14 and 1.30×10^{-13} m^2W^{-1}, respectively. The attenuation coefficient of the waveguide is 0.1 dB $(mm)^{-1}$. The multiplexed signals can be applied via the add port, in which the secure bits can be performed by the soliton control.

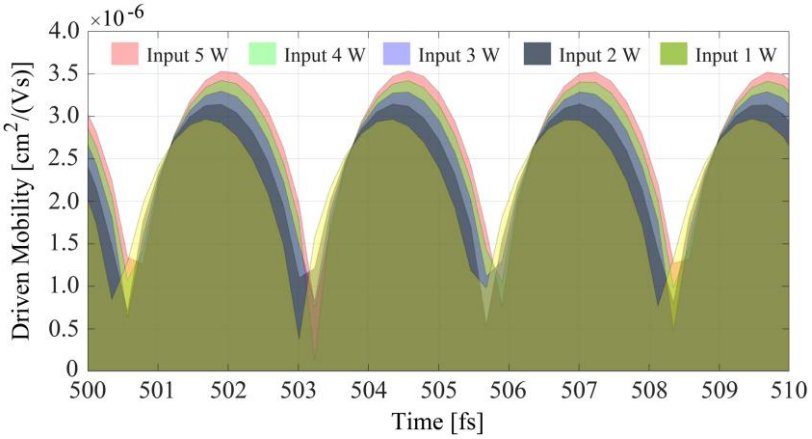

Figure 5: The plots of the mobility output at the Island, where the add port input is the bright soliton pulse, the peak power is 1 W, the input soliton pulse peak power is ranged from 1-5 W.

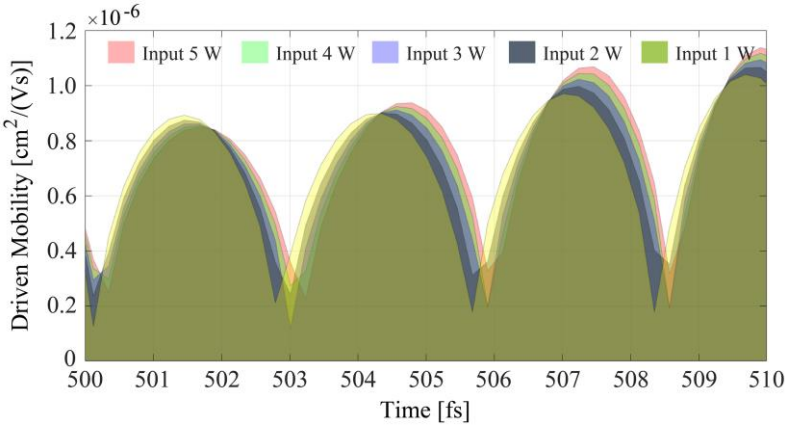

Figure 6: : The plots of the mobility output at the Island, where the add port input is the Gaussian pulse, with a peak power is 1 W, the input soliton pulse peak power is ranged from 1-5 W.

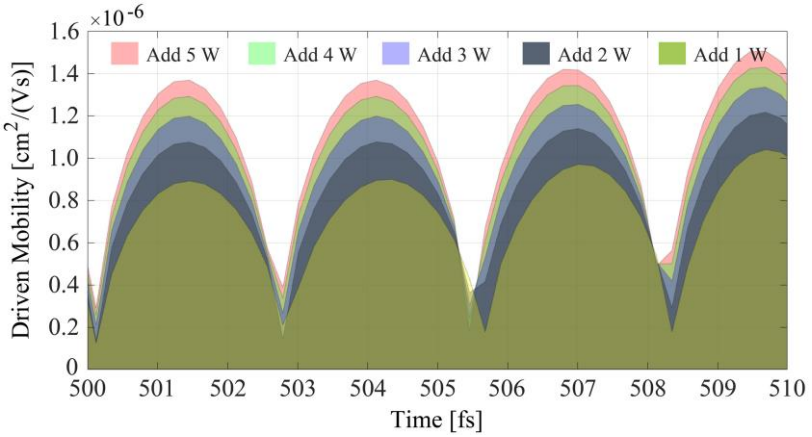

Figure 7: The plots of the mobility output at the Island, where the input soliton pulse peak power is 1 W and the add port input is the Gaussian pulse, the peak power is ranged from 1-5 W.

4. Conclusion

The ultrafast electro-optic switching using a modified add-drop optical filter is designed and modelled for electro-optic flip-flop application. The bright soliton is the input source that is input into the system via the input port. The output at the throughput and drop ports can be used to form the switching signals as "On" or "Off" randomly, which is the soliton output characteristics via a 3 dB coupler. The control signal is input into the system via an add port, which can be another common laser having the same wavelength as the fiber laser(soliton) put. It provides the security codes for transmission. The light signal is converted into the electronic signal by the plasmonic stacked layers which are placed on the certain length at the device ends. The major advantages are the ultrafast flip-flop speed and the secure signals achieved by the soliton dark-bright conversion behaviors and the ultrafast switching speed. The secure transmission is formed the control port signal that allows the dark/bright output signals to be identified between the sender and receiver. The simulation results obtained have shown that the time offset is 220 fs with a half-width of 5 fs, the center wavelength is 1.55 μm with a spectral width of 450 nm at FWHM, (b) the input and add port with the soliton pulses of 1 W with a center wavelength of 1.55 μm and 60 nm spectral width at FWHM, which is the interesting for electronic flip-flop switching time. Moreover, there are two alternative transmission techniques, a free space and optical fiber links can be applied.

Acknowledgments

The authors would like to give the appreciation for the research financial support by GUP project (Tier2 15J57) and Flagship UTM Shine Project (03G82) to the Universiti Teknologi Malaysia, Johor Bahru, Malaysia. One of the authors “S. Soysouvanh” would like to give an acknowledgement to AUN-SEED-Net for a scholarship support in PhD program.

References

[1] Pornsuwancharoen N, Amiri IS, Suhailin FH, Aziz MS, Ali J, Singh G, Yupapin P.(2017), Micro-current source generated by a WGM of light within a stacked silicon-graphene-Au waveguide, IEEE Photon. Technol. Lett., 19, 1768-1771.

[2] S.J. Kim, M.J. Park, D.J. Yun, W.H. Lee, G.H. Kim, S.M. Yoon, High performance and stable flexible memory thin-film transistor using In-Ga-Zn-O channel and ZnO charge-trap layers on poly(Ethylene Naphthalate) substrate, IEEE Transaction on Electron Devices, 63(4), 1557-1564.

[3] A. Agrawal, M. Tiwari, Y.O. Azabi, V. Janyani, B.M.A. Rahman and K.T.V. Grattan,” Ultrabroad supercontinuum generation in tellurite equiangular spiral photonic crystal fiber”, J. of Mod. Opt. 60 (12), 956-962(2013).

[4] P. Youplao, N. Sarapat, N. Pornsuwancharoen, K. Chaiwong, M.A. Jalil, I.S. Amiri, M.S. Aziz, S. Chiangga, G. Singh, P. Yupapin, K.T.V. Grattan, Plasmonic op-amp circuit model using the inline successive microring pumping technique, Microsystem technologies, online, pp. 1-7, 2018.

[5] M. Zhang, Y. Wang, P. Li, H. Wen, Comparative studies on two electromagnetic repulsion mechanisms for high-speed vacuum switch, IET Electric Power Applications, 12(2), pp. 247-253.

[6] X. Xiao, Y. Xu, H. Guo, P. Wang, X. Cui, M. Lu, Y. Wang, B. Peng, Theoretical modeling of 4.3 μm mid-infrared lasing in Dy3+doped chalcogenide fiber lasers, IEEE Photonics Journal, 10(2), Article number 1501011, 2018.

[7] N.T. Kejalakshmy, K.T.V Grattan, B.M.A. Rahman, Investigate of the optical modal properties of Al+3 Doped ZnO-Coated Au Waveguide for Gas Sensing Applications Using the Finite Element Method, IEEE Sensors Journal, 16(5), pp. 1176-1181, 2016.

[8] C. Ning, J. Jin, K. Yang, H. Xie, D.W. Wang, Y. Liao, L.D. Wang, H.S. Chen, E.P. Li, W.Y. Yin, A novel electromagnetic bandgap power plane etched multiring CSRRs for suppressing simultaneous switching noise, IEEE Transactions on Electromagnetic Compatibility, 60(3), pp. 733-737, 2018.

[9] H. Chen, R. Nie, M. Sun, W. Deng, K. Liang, 3-D electromagnetic analysis of single-phase tubular switched reluctance linear launcher, IEEE Transactions on Plasma Science, 45(7), pp. 1553-1560, 2017.

[10] Y. Hu, W. Ding, T. Wang, S. Li, S. Yang, Z. Yin, Investigation on a multimode switched reluctance motor: design, optimization, electromagnetic analysis, and experiment, IEEE Transactions on Industrial Electronics, 64(12), pp. 9886-9895, 2017.

[11] Z.D. Khedda, K. Boughrara, F. Dubas, R. Ibtiouen, Nonlinear analytical prediction of the magnetic field and electromagnetic performances in switched reluctance machines, IEEE Transactions on Magnetics, 53(7), Article number 8107311, 2017.

[12] W. Hafez, M. Feng, Experimental demonstration of pseudomorphic heterojunction bipolar transistors with cutoff frequencies above 600 GHz, Applied Physics Letters, 86(15), Article number 152101, 2005.

[13] A. Kowsari, H. Saghaei, Resonantly enhanced all-optical switching in microfibre Mach-Zehnder interferometers, Electronics Letters, 54(4), pp. 229-231, 2018.

[14] K. Sato, Realization and application of large-scale fast optical circuit switch for data center networking, Journal of Lightwave Technology, 36(7), pp. 1411-1419.

[15] M.R. Shcherbakov, P.P. Vabishchevich,A.S. Shorokhov, K.E. Chong, D.Y. Choi, S. Staude, A.E. Miroshnichenko, D.N. Neshev, A.A. Fedyanin, and Y.S. Kivshar, Ultrafast All-Optical Switching with Magnetic Resonances in Nonlinear Dielectric Nanostructures, Nano Letters, 15, 6985−6990, 2015.

[16] Al, J., Pornsuwancharoen, P., Youplao, P., Amiri, I.S., Chaiwong, K., Chiangga, S., Singh, G. and Yupapin, P. 2018, Coherent light squeezing states within a modified microring system, Results in Physics, online, pp. 1-4, 2018.

[17] Pornsuwancharoen, N., Youplao, P., Aziz, M.S., Ali, J., Amiri, I.S., Punthawanunt, S., Yupapin, P. and Grattan, K.T.V. 2018, In-situ 3D micro-sensor model using the embedded plasmonic island for biosensors, Microsystem Technologies, online, pp. 1-7, 2018.

[18] Pornsuwancharoen, N., Youplao, P., Aziz, M.S., Ali, J., Singh, G., Amiri, I.S., Punthawanunt, S., Yupapin, P. 2018, Characteristics of microring circuit using plasmonic island driven electron mobility, Microsystem Technologies, online, pp. 1-5, 2018.

[19] Amiri, I.S., Ali, J. and Yupapin, P.P. 2012, Enhancement of FSR and finesse using add/drop filter and panda ring resonator, J. Mod. Phys. B 26, 1250034.
[20] Phatharaworamet, T., Teeka, C., Jomtarak, R., Mitatha, S. and Yupapin, P.P., 2010. Random binary code generation using dark-bright soliton conversion control within a Panda Ring resonator, J Lightwave Technol., 28(19), 2804-2809.
[21] Phattharacorn, P., Chiangga, S., Ali, J. And Yupapin, P., 2018, Micro-optical probe model using integrated triple microring resonators for vertical depth identification, Microsystem and Technologies, online, pp- 1-7, 2018.
[22] Pornsuwancharoen N, Youplao P, Amiri IS, Ali J, Yupapin P (2017), Electron driven mobility model by light on the stacked metal-dielectric-interfaces, Microw. & Opti. Techn. Lett., 59, 1704-1709.
[23] Gall, D. 2016, Electron mean free path in elemental metals, J Appl. Phys., 119, 085101.
[24] Baccarani, G. and Ostoja, P. 1975, Electron mobility empirically related to the phosphorus concentration in silicon, Solid State Electron., 18(6), 579-580.